

Supporting Information

Nuclei position-control and crystal growth-guidance on frozen substrate for high performance perovskite solar cell

Gang Wang ^{a, b, †}, Liping Liao ^{a, b, †}, Lianbin Niu ^c, Lijia Chen ^c, Wenjun Li ^b, Cunyun Xu ^{a, b}, Elisabeth Mbeng ^{a, b}, Yanqing Yao ^{a, b}, Debei Liu ^{a, b}, Qunliang Song ^{a, b, *}

^aInstitute for Clean Energy and Advanced Materials, School of Materials and Energy, Southwest University, Chongqing 400715, P. R. China

^bChongqing Key Laboratory for Advanced Materials and Technologies of Clean Energy, Chongqing 400715, P. R. China

^cCollege of Physics and Electronics Engineering, Chongqing Normal University, Chongqing 401331, P. R. China

[†] Those author contributed equally to this work.

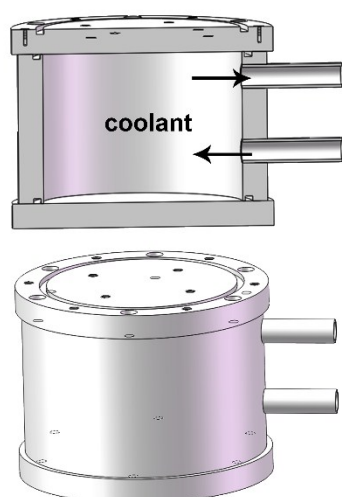


Figure S1. The design and the photo of the home-made cooling system for NPCG method. The cooling plate is placed near the spin coater in the same glove box.

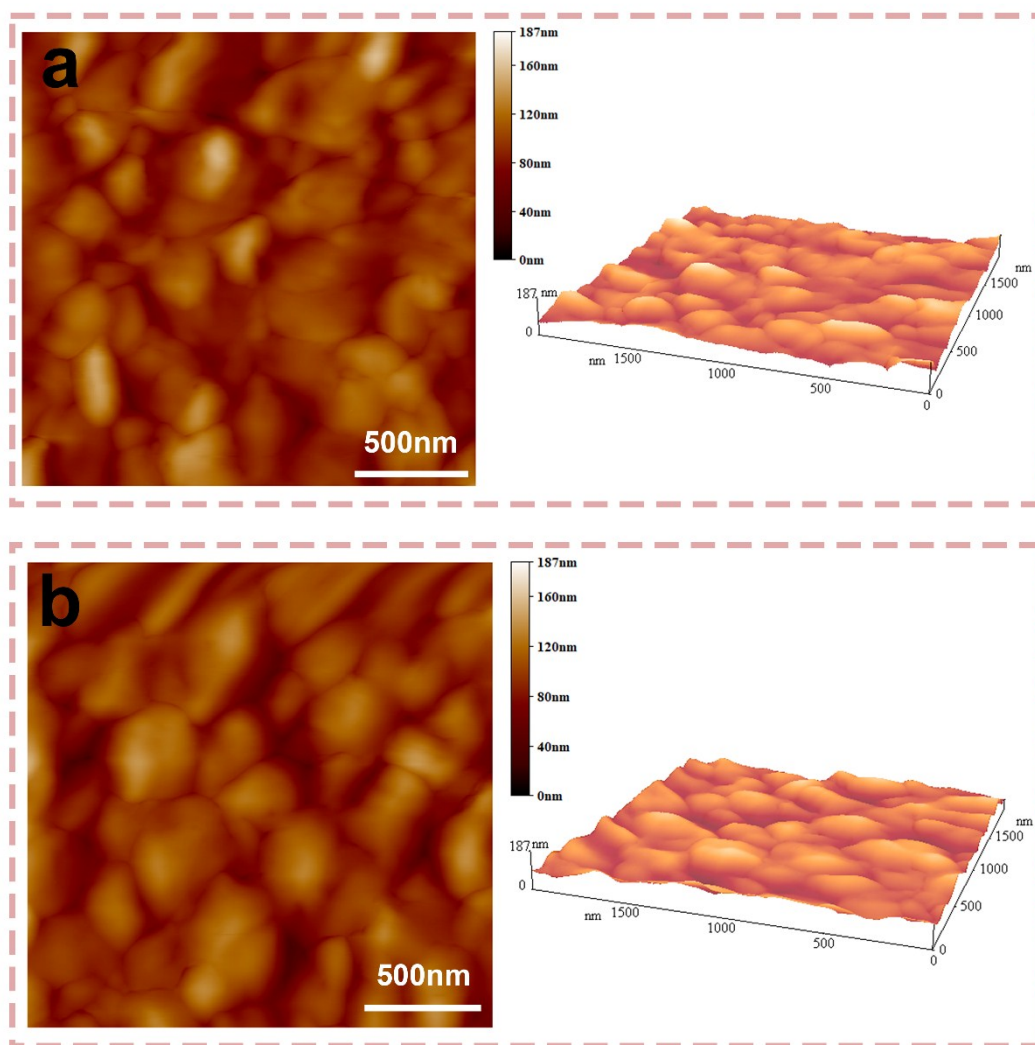


Figure S2. AFM images for RT (a) and NPCG@0 (b) perovskite films after thermal annealing at 85 °C for 30 minutes.

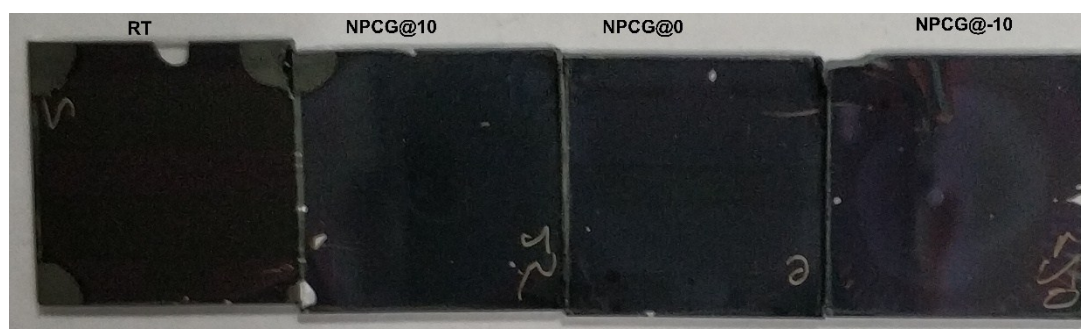


Figure S3. Photos of perovskite films (back) fabricated by RT and NPCG methods before depositing ETL and cathode.

Table S1. Photovoltaic performance of PSCs fabricated with different substrate temperatures in the same batch.

PSCs	V_{oc} (V)	J_{sc} ($\text{mA}\cdot\text{cm}^{-2}$)	FF (%)	PCE (%)
NPCG@-10	1.13	20.11	69.03	15.64
NPCG@0	1.12	20.22	71.21	16.13
NPCG@10	1.12	19.89	70.83	15.74
RT	1.07	18.78	72.33	14.53

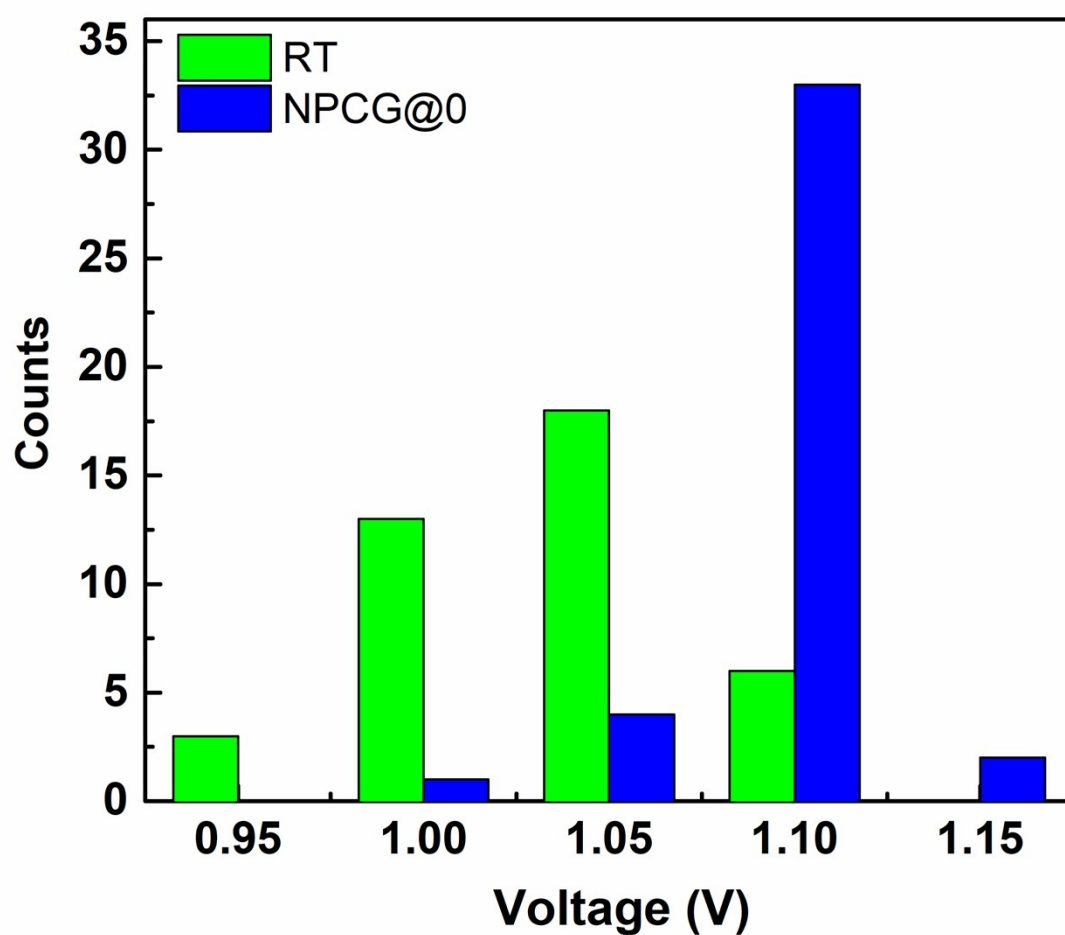


Figure S4. Statistical V_{oc} of 40 PSC devices for RT and NPCG@0 method respectively.

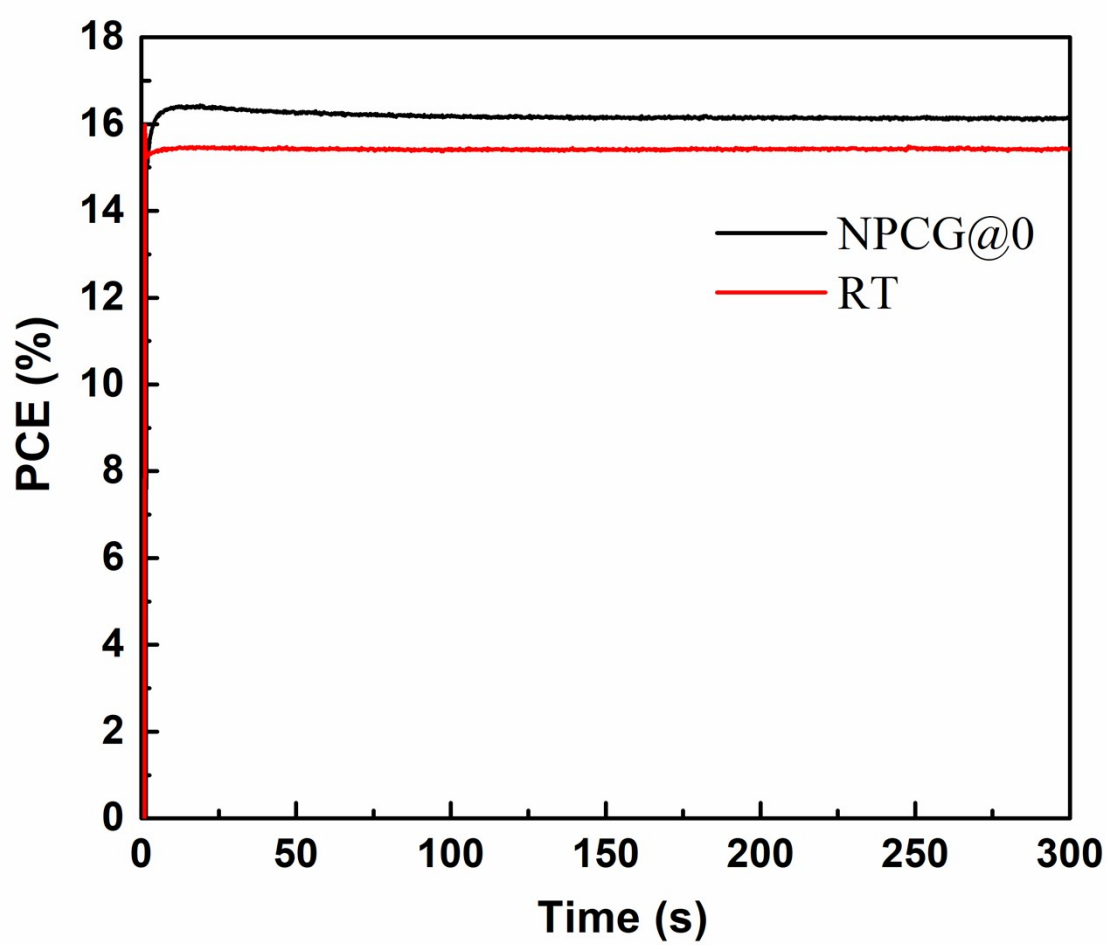


Figure S5. The steady output at the maximum power point for NPCG@0 and RT devices.